

Neural network analysis of steel plate processing

S. B. Singh, H. K. D. H. Bhadeshia, D. J. C. MacKay, H. Carey, and I. Martin

The process of rolling is very complicated and the number of parameters which determines the final properties can be quite large. It is extremely difficult therefore to develop a physical model for predicting various properties like yield and tensile strengths. In the present work, a neural network technique which can recognise complex relationships was employed to develop a quantitative method for estimating the yield and tensile strengths as a function of steel composition and rolling parameters. The model was tested extensively to confirm that the predictions are reasonable in the context of metallurgical principles and other data published in the literature.

IS/1355

© 1998 The Institute of Materials. Manuscript received 13 January 1998. Dr Singh and Dr Bhadeshia are in the Department of Materials Science and Metallurgy, University of Cambridge, Cambridge, Dr MacKay is at the Cavendish Laboratory, Cambridge, and Dr Carey and Dr Martin are with British Steel plc, Swinden Technology Centre, Rotherham, South Yorkshire.

INTRODUCTION

Cast steel is usually processed into usable products by severe plastic deformation, frequently using the rolling process. The purpose of this deformation is to refine the cast microstructure, to produce the steel in the required shape, and to achieve the optimum mechanical properties. The properties depend not only on the deformation but also on the detailed chemical composition in two respects. First, the steel may contain microalloying elements which help control the austenite grain structure and in some cases provide precipitation strengthening.¹ The other alloying additions such as manganese control the relative stabilities of the austenite and ferrite phases and hence the nature of the austenite transformation products.

When a hot ingot or slab enters a rolling mill, its typical dimensions are so large that it has to be reduced to the required thickness in many separate passes. The purpose of the present work was to develop a model enabling the estimation of strength as a function of a large number of rolling parameters and the chemical composition of the steel. The model is based on the neural network analysis technique with a total of 108 variables; the method and the variables are introduced below. The work is restricted to steels with a ferrite and pearlite microstructure.

TECHNIQUE

Neural networks are parametrised non-linear models used for empirical regression and classification modelling. Their flexibility makes them able to discover more complex relationships in data than traditional linear statistical models.

A neural network is 'trained' on a set of examples of input and output data. The outcome of this training is a set of coefficients (called weights) and a specification of the functions which in combination with the weights relate the

input to the output. The training process involves a search for the optimum non-linear relationship between the inputs and the outputs and is computer intensive. Once the network is trained, the estimation of the outputs for any given inputs is very rapid. The details of the method used here have recently been comprehensively reviewed² and the original method is described in Refs. 3-7.

One of the difficulties with blind data modelling is that of 'overfitting', in which spurious details and noise in the training data are overfitted by the model. This gives rise to solutions that generalise poorly. MacKay³⁻⁷ and Neal⁸ have developed a Bayesian framework for neural networks in which the appropriate model complexity is inferred from the data.

The Bayesian framework for neural networks has two further advantages. First, the significance of the input variables is quantified automatically. Consequently the model perceived significance of each input variable can be compared against metallurgical theory. Second, the network's predictions are accompanied by error bars which depend on the specific position in input space. These quantify the model's certainty about its predictions.

DATABASE

The neural network method is empirical and hence requires experimental data to discover the relationships. The data used were obtained directly from an actual commercial, instrumented plate rolling mill. Given that the work is focused on the production mill, the variables have to be selected from routine records. The input variables therefore consisted of:

- (i) the slab reheating temperature, which is universally recognised to be important in determining the initial austenite grain size and the temperature of the slab as it progresses through the rolling mill
- (ii) the length of the slab, which determines the timing of the rolling process
- (iii) the slab gauge; this is of vital importance in determining the total reduction required to achieve the final plate thickness
- (iv) the chemical composition, consisting of a total of 14 different elements
- (v) the rolling parameters, including the pass by pass screw settings, any delay period between the passes, and the time spent for an individual pass
- (vi) the 'rolling condition' which is set to 0 for as rolled plates and 1 for control rolled or normalised rolled plates; the latter involved rolling with water cooling, with or without a delay period.

A total of 1892 examples were available for analysis. The maximum number of rolling passes is 30; when the number is less than 30, the missing passes were set with zero pass time, zero delay time, and with a roll gap setting which gives zero deformation. The purpose of the analysis was to be able to estimate the yield and ultimate tensile strengths as a function of each of the 108 variables. Some further information about the variables is given in Table 1; that information is necessary to reproduce the present work using the trained network.

ANALYSIS

Both the input and output variables were first normalised within the range ±0.5 as follows

$$x_N = \frac{x - x_{min}}{x_{max} - x_{min}} - 0.5 \quad (1)$$

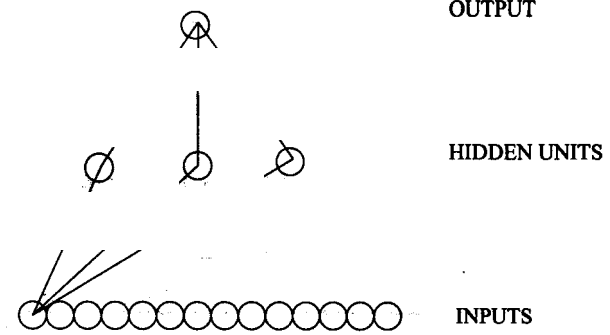
where x_N is the normalised value of x which has maximum and minimum values given by x_{max} and x_{min} , respectively.

Linear functions of the inputs x_j are operated on by a hyperbolic tangent transfer function

$$h_i = \tanh \left[\sum_j w_{ij}^{(1)} x_j + \theta_i^{(1)} \right] \quad (2)$$

so that each input contributes to every hidden unit (Fig. 1). The bias is designated θ_i and is analogous to the constant that appears in linear regression. The strength of the transfer function is in each case determined by the weight w_{ij} . The transfer to the output y is linear

$$y = \sum w_{ij}^{(2)} h_i + \theta^{(2)} \quad (3)$$

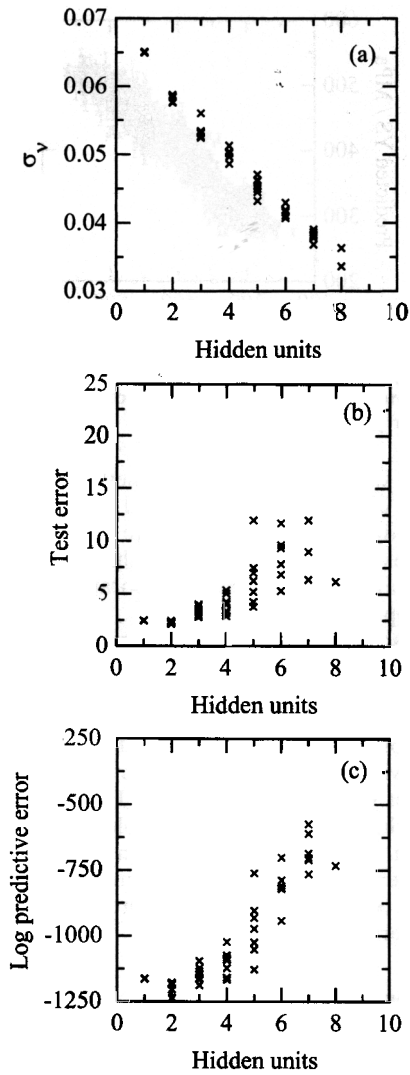


1 Typical network used in analysis; only connections originating from one input unit are shown, and two bias units are not shown

The specification of the network structure, together with the set of weights, is a complete description of the formula relating the inputs to the output. The weights are determined

Table 1 Variables, with concentrations stated in wt-%: $S(J)$ = screw setting, mm, for J th pass; $D(J)$ = delay time, s, before J th pass; $T(J)$ = J th pass time

Variable	Range	Mean	Standard deviation	Variable	Range	Mean	Standard deviation
Reheating temperature, °C	993-1373	1212	22.98	T(13)	0.0-15.0	5.0	2.41
Slab gauge, mm	161-600	245.1	36.25	S(14)	5.8-167.2	43.7	22.85
Slab length, mm	915-4080	2828	700.6	D(14)	0.0-163.0	6.3	6.03
C	0.076-0.25	0.14	0.036	T(14)	0.0-28.0	5.3	2.98
Mn	0.7-1.54	1.29	0.24	S(15)	7.0-780.0	40.5	20.75
Si	0.14-0.46	0.32	0.07	D(15)	0.0-790.0	20.6	84.70
S	0.001-0.019	0.006	0.004	T(15)	0.0-15.0	4.7	3.04
P	0.008-0.027	0.015	0.003	S(16)	5.3-157.1	38.0	19.33
Ni	0.014-0.56	0.038	0.045	D(16)	0.0-163.0	5.9	8.02
Cr	0.01-0.53	0.028	0.047	T(16)	0.0-26.0	5.0	3.62
Mo	0.001-0.017	0.003	0.0014	S(17)	7.7-153.8	36.3	17.91
Cu	0.004-0.296	0.032	0.049	D(17)	0.0-497.0	6.5	19.64
Al	0.0-0.058	0.036	0.008	T(17)	0.0-17.0	3.9	3.42
Nb	0.0-0.11	0.005	0.002	S(18)	7.9-151.3	34.9	16.98
N	0.0-0.043	0.024	0.014	D(18)	0.0-111.0	4.9	7.43
V	0.001-0.063	0.009	0.016	T(18)	0.0-21.0	4.2	4.12
Ti	0.0-0.033	0.0019	0.0017	S(19)	7.9-150.2	33.9	16.17
S(1)	91.0-354.9	190.3	40.67	D(19)	0.0-193.0	4.3	8.14
D(1)	47.0-736.0	144.3	58.05	T(19)	0.0-17.0	3.1	3.72
T(1)	1.0-3.0	1.5	0.51	S(20)	7.9-150.2	33.1	15.57
S(2)	80.1-343.1	175.4	39.75	D(20)	0.0-86.0	4.1	7.74
D(2)	5.0-39.0	7.3	1.77	T(20)	0.0-27.0	3.1	4.02
T(2)	1.0-5.0	2.2	0.92	S(21)	7.9-150.2	32.5	15.16
S(3)	66.1-328.1	161.1	38.44	D(21)	0.0-183.0	4.2	14.35
D(3)	5.0-105.0	14.4	10.34	T(21)	0.0-15.0	2.4	3.66
T(3)	1.0-25.0	1.5	0.75	S(22)	7.6-150.2	32.1	14.87
S(4)	64.5-311.2	150.0	37.02	D(22)	0.0-142.0	3.4	8.78
D(4)	4.0-198.0	12.6	6.58	T(22)	0.0-19.0	2.4	3.78
T(4)	1.0-6.0	2.4	1.19	S(23)	7.6-150.2	31.8	14.72
S(5)	46.0-288.6	130.6	36.43	D(23)	0.0-172.0	4.4	16.45
D(5)	5.0-1163.0	48.4	160.24	T(23)	0.0-16.0	1.8	3.40
T(5)	1.0-9.0	2.0	0.80	S(24)	7.9-150.2	31.5	14.60
S(6)	34.4-268.0	119.1	36.66	D(24)	0.0-121.0	2.2	6.60
D(6)	3.0-263.0	10.0	8.24	T(24)	0.0-14.0	1.7	3.35
T(6)	1.0-9.0	2.6	0.87	S(25)	7.9-150.2	31.4	14.45
S(7)	26.8-249.1	103.9	35.99	D(25)	0.0-295.0	2.9	15.97
D(7)	5.0-986.0	72.1	181.24	T(25)	0.0-13.0	1.2	2.81
T(7)	1.0-5.0	2.5	0.91	S(26)	7.9-50.2	31.3	14.38
S(8)	21.3-232.1	92.2	35.66	D(26)	0.0-107.0	1.6	6.19
D(8)	4.0-43.0	8.0	3.66	T(26)	0.0-15.0	1.2	3.12
T(8)	1.0-7.0	3.1	1.03	S(27)	7.9-150.2	31.2	14.30
S(9)	15.7-216.9	79.3	33.20	D(27)	0.0-112.0	1.1	5.60
D(9)	0.0-894.0	102.1	218.45	T(27)	0.0-13.0	0.7	2.21
T(9)	0.0-48.0	3.4	1.67	S(28)	6.7-150.2	31.2	14.29
S(10)	12.9-203.5	69.3	31.32	D(28)	0.0-136.0	1.3	7.50
D(10)	0.0-170.0	6.7	5.28	T(28)	0.0-15.0	0.5	2.05
T(10)	0.0-19.0	4.0	1.71	S(29)	7.9-150.2	31.2	14.25
S(11)	11.1-192.0	60.3	28.94	D(29)	0.0-40.0	0.4	2.02
D(11)	0.0-910.0	41.8	128.62	T(29)	0.0-12.0	0.2	1.05
T(11)	0.0-16.0	4.4	1.81	S(30)	7.2-150.2	31.1	14.25
S(12)	8.8-182.4	53.5	26.97	D(30)	0.0-64.0	0.5	4.57
D(12)	0.0-660.0	7.0	17.71	T(30)	0.0-10.0	0.1	0.92
T(12)	0.0-20.0	4.9	2.19	Condition	0 or 1		
S(13)	8.0-174.0	47.9	24.65	Yield strength, MPa	232.0-594.0	398.5	66.64
D(13)	0.0-735.0	24.0	84.84	Ultimate tensile strength, MPa	389-692	537.5	44.07



a variation in σ_v as function of number of hidden units; b test error for each model; c log predictive error

2 YS model (several values are presented for each set of hidden units because training for each network was started with variety of random seeds)

by training the network; the details are described elsewhere.³⁻⁷ The training involves a minimisation of the regularised sum of squared errors. The term σ_v used below is the framework estimate of the noise level of the data.

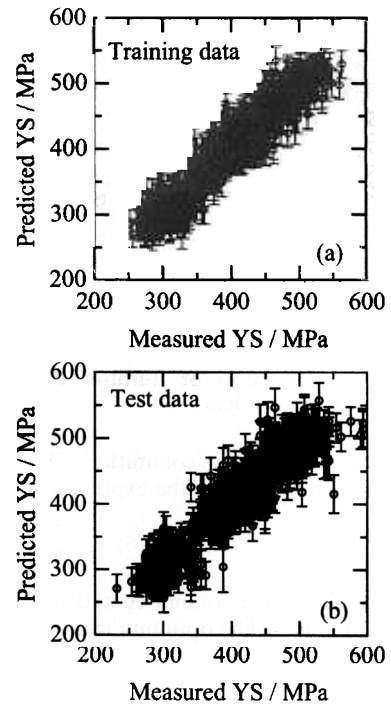
NETWORK TRAINING

Yield strength

The network model for the yield strength consisted of 108 input nodes, a number of hidden nodes, and an output node representing the yield strength. The network was trained using 946 of the examples randomly chosen from a total of 1892 available, the remaining 946 examples being kept aside at first to be used as 'new' experiments to test the behaviour of the trained network.

The complexity of the model is controlled by the number of hidden units (Fig. 2), and the values of the 110 regularisation constants σ_w , one associated with each of the 108 inputs, one for biases, and one for all weights connected to the output.

Figure 2a shows that the inferred noise level decreases as the number of hidden units increases. However, the complexity of the model also increases with the number of hidden units. A high degree of complexity may not be justified and, in an extreme case, the model may in a



3 Comparison between predicted and measured YS for training and test data; error bars are set to $\pm 1\sigma$ limits and have two components: error bar on underlying function and inferred noise level in data for this model σ_v

meaningless way attempt to fit the noise in the experimental data. The number of hidden units was set by examining the performance of the model on the unseen test data (Fig. 2b). A combination of Bayesian and pragmatic statistical techniques were therefore used to control the model complexity. Test error T_e is a measure of the deviation of the predicted value from the experimental one in the test data

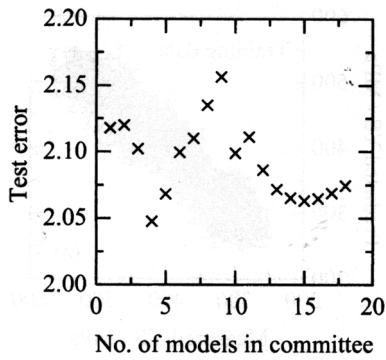
$$T_e = 0.5 \sum_n (y_n - t_n)^2 \dots \dots \dots (4)$$

where y_n is the predicted yield strength and t_n is its measured value.

It is seen that a model with just two hidden units gives an adequate representation of the data with a minimum in the test error (Fig. 2b). The behaviour of the training and test data is shown in Fig. 3 which shows a similar degree of scatter in both the graphs, indicating that the complexity of this particular model is optimum. It should be noted that the test data cover a wider range of yield strength values and, for a few cases at the highest yield strengths, the model underpredicts the measured values. Overfitting would lead to an apparently better accuracy in the prediction of training data when compared with the test dataset. The error bars in Fig. 3 include the error bars on the underlying function and the inferred noise level in the dataset σ_v . In all other subsequent predictions discussed below the error bars include the former component only. The test error is one measure of the performance of a model. Another useful measure is the 'log predictive error'³⁻⁶ for which the penalty for making a wild prediction is much less if the wild prediction is accompanied by an appropriately large error bar. Assuming that for each example n the model gives a prediction with error (y_n, σ_n^2) , the log predictive error (LPE) is

$$LPE = \sum_n \left[\frac{\frac{1}{2}(t_n - y_n)^2}{\sigma_n^2} + \log(\sqrt{2\pi}\sigma_n) \right] \dots \dots \dots (5)$$

When making predictions, MacKay⁵ has recommended the use of multiple good models instead of just one best model.



Test error as function of number of members in committee of YS models

This is called 'forming a committee'. The committee prediction \bar{y} is obtained using the expression

$$\bar{y} = \frac{1}{L} \sum_i y_i \quad \dots \dots \dots (6)$$

where L is the size of the committee and y_i is the estimate of a particular model i . The optimum size of the committee is determined from the validation error of the committee's predictions using the test dataset. The test error of the predictions made by a committee is calculated by replacing the y_n in equation (4) with \bar{y} . In the present analysis a committee of models was used to make more reliable predictions. The models were ranked according to their log predictive error. Committees were then formed by combining the predictions of best M models, where M gives the number of members in a given committee model. The test errors for the first 18 committees are shown in Fig. 4.

A committee of the best four models gives the minimum error; three of these were two hidden unit models and the remaining one was a three hidden unit model. Each constituent model of the committee was therefore retrained on the entire dataset beginning with the weights previously determined. Figure 5 shows the results from the new training on the entire dataset. For the sake of simplicity, the error bars in Fig. 5 include the error on the fitted function only.

Ultimate tensile strength

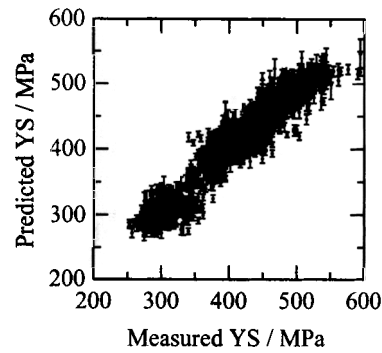
The same procedure was used to model the ultimate tensile strength (UTS), with the same set of 108 input variables. The variation in σ_v , the test error, and log predictive error with the number of hidden units is shown in Fig. 6.

The model with two hidden units was found to be the optimum one and a committee of the nine best models led to a further reduction in the test error, as shown in Fig. 7.

The results of the retraining of the committee model on all of the data are shown in Fig. 8.

APPLICATION OF MODELS

The optimised committee models were used to study the effect of individual variables on the yield strength and



5 Training data for best YS committee model (training was done on whole dataset); error bars include error in underlying function only

the tensile strength to find out whether the results are compatible with known metallurgical principles and other published data. These studies are limited to simple relationships since there are no metallurgical models which deal with all the variables incorporated in the neural network approach.

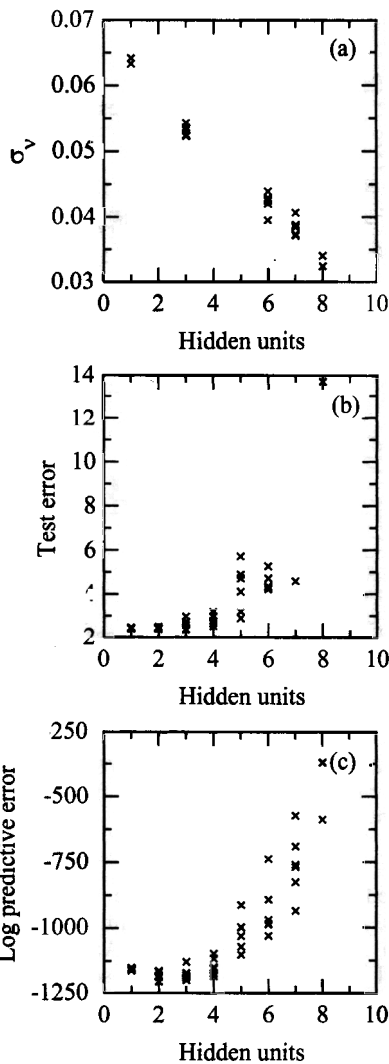
In the discussion that follows, a typical 19 pass schedule with a starting slab thickness of 200 mm and the final pass screw setting of 13.8 mm was used unless otherwise stated. The slab reheating temperature was set at 1215°C. The chemical compositions were set at their average concentrations given in Table 1. A comprehensive list of the standard set of variables is given in Table 2 in the precise order in which they appear in Table 1. For example, a variation in the carbon concentration is discussed leaving all the other variables in Table 2 unchanged. In all the predictions below, the error bars represent the $\pm 1\sigma$ limits on the underlying function.

Carbon concentration

It is well known that carbon forms an interstitial solid solution in iron, leading to intense solid solution strengthening. The effect is more pronounced in the case of ferritic iron because, unlike austenite, the carbon atoms cause a tetragonal distortion of the lattice giving strong interactions with all kinds of dislocations.⁹ It has been estimated that 1 wt-%C in solid solution in ferrite raises the yield strength by 4600 MPa and UTS by 6800 MPa (Ref. 10). However, the solubility of carbon in ferrite is extremely small so that the main effect in the context of steels with a mixed microstructure of ferrite and pearlite is to increase the fraction of the latter phase. There is also a refinement of microstructure since the temperature at which the ferrite forms is suppressed. Both the yield and tensile strengths should therefore increase with the carbon concentration and this is indeed replicated by the model (Fig. 9); the calculations are for a steel without Nb or V additions. Note also that, as must be expected, the UTS is always predicted to be higher than the yield strength even though the latter was not included as an input to the UTS model. The error bars ($\pm 1\sigma$) are larger when an attempt is made

Table 2 Variables used for predictions; these variables appear in same sequence as in Table 1

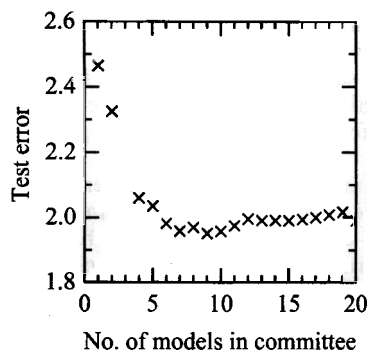
1215.0	200.0	2760.0	0.140	1.260	0.320	0.007	0.015	0.031
0.030	0.003	0.025	0.037	0.005	0.023	0.009	0.002	174.0
158.0	2.0	149.6	8.0	4.0	141.3	23.0	1.0	133.6
7.0	1.0	125.9	6.0	2.0	118.3	5.0	2.0	110.0
6.0	2.0	105.1	16.0	3.0	85.1	24.0	3.0	70.7
7.0	3.0	58.6	6.0	3.0	48.7	7.0	3.0	40.1
7.0	4.0	33.0	6.0	5.0	22.9	36.0	6.0	15.8
7.0	9.0	14.9	6.0	9.0	14.1	7.0	10.0	13.8
7.0	10.0	13.8	0.0	0.0	13.8	0.0	0.0	13.8
0.0	0.0	13.8	0.0	0.0	13.8	0.0	0.0	13.8
0.0	0.0	13.8	0.0	0.0	13.8	0.0	0.0	13.8
0.0	0.0	13.8	0.0	0.0	13.8	0.0	0.0	7



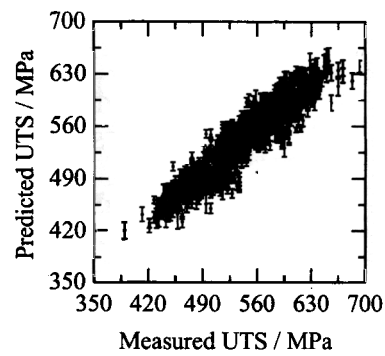
6 σ_v and errors as function of number of hidden units for UTS models (several values are presented for each set of hidden units because training for each network was started with variety of random seeds)

to predict at concentrations beyond the range of the training dataset. The yield strength increases by about 32 MPa (ignoring the error bars) when the concentration is increased from 0.025 to 0.25 wt-%. This is consistent with experimental data by Hodgson and Gibbs¹¹ who found an increase in the lower yield strength by about 15 MPa for a 0.1 wt-% increase in the carbon concentration.

Consistent with experimental observations,^{10,12,13} the UTS is predicted to be more sensitive to the carbon



7 Test error as function of number of members in committee of models for UTS



8 Training data for best UTS committee model (training was done on whole dataset)

concentration than the yield strength (Fig. 9). The predominant effect of carbon in the steels considered here is to increase the pearlite fraction in the microstructure. For carbon concentrations up to 0.3 wt-% where the pearlite fraction is relatively small, yielding begins in the softer ferrite which has to work harden before the pearlite starts to undergo plastic deformation. As a consequence, the effect of pearlite on the yield strength is smaller. On the other hand, pearlite content does affect the UTS because it is associated with large plastic strains where all phases must participate in deformation. These observations are also reflected in Pickering's¹⁰ regression equations for similar steels, where the quantity of pearlite features only in the UTS equation

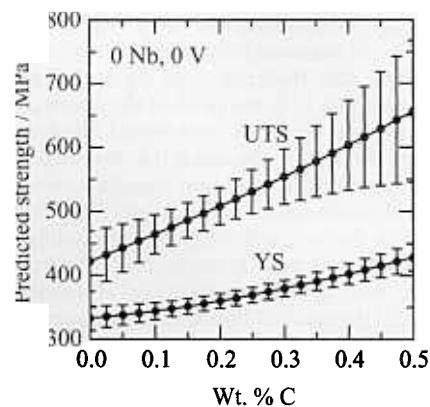
$$YS, \text{ MPa} = 53.9 + 32.3w_{Mn} + 83.2w_{Si} + 354.2w_{N_f}^{0.5} + 17.4d^{-0.5} \dots \dots \dots (7)$$

$$UTS, \text{ MPa} = 294.1 + 27.7w_{Mn} + 83.2w_{Si} + 3.85(\% \text{ pearlite}) + 7.7d^{-0.5} \dots \dots (8)$$

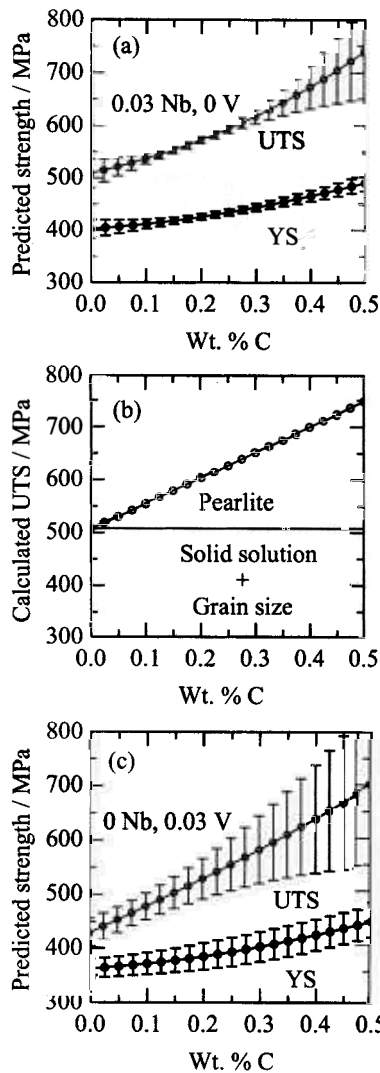
where w represents the concentration of the element identified by the subscript (in weight per cent) N_f is the free nitrogen, and d is the ferrite grain size in millimetres.

Based on a study covering a wide range of ferrite grain sizes in a number of carbon steels, Morrison¹⁴ found a slightly different factor of 18.13 for the effect of ferrite grain size on the yield strength (equation (7)).

Figure 10a shows calculations for a microalloyed steel with 0.03 wt-%Nb. Figure 10b shows, on the same scale, the effect of increasing pearlite content on the UTS as calculated using equation (8) – the zero carbon result is from the neural network model. The agreement between the two is excellent and similar results have been reported by Shimizu *et al.*¹²



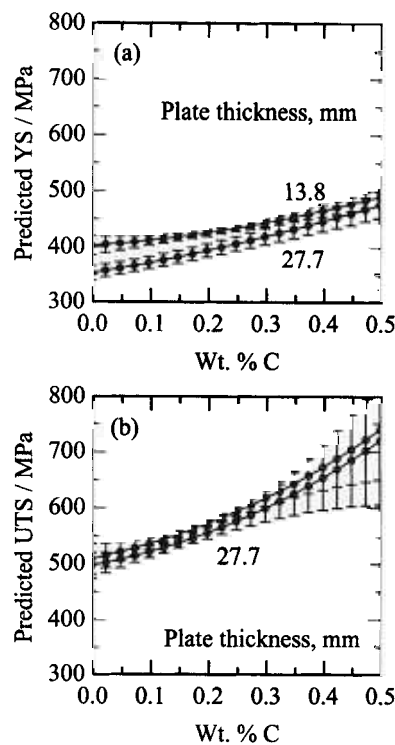
9 Variation of YS and UTS with carbon for steel without any microalloying additions; error bars represent $\pm 1\sigma$ limits



10 *a* Effect of carbon and *b* effect of pearlite content on YS and UTS of microalloyed steel containing 0.03 wt-%Nb (zero V) and *c* YS and UTS for 0.03 wt-%V microalloyed steel (zero Nb); other elements were as in Table 2; UTS in *b* was calculated using equation (8)¹⁰

A comparison of Figs. 9 and 10*a* shows that the addition of 0.03 wt-%Nb to a plain C-Mn steel increases both the yield and ultimate tensile strengths by about 65 MPa at all carbon concentrations. A corresponding addition of 0.03 wt-%V increases the strength by only about 20 MPa (Fig. 10*c*). It is well known that niobium is more effective in restricting recrystallisation than vanadium.^{15,16} The reason for this is discussed separately.

The starting slab thickness was set at 200 mm and the final plate thickness 13.8 mm in all of the above calculations. If this is changed to a 400 mm initial thickness but the rolling schedule is kept the same (i.e. the same percentage pass reductions and the pass and interpass times), then the final plate thickness becomes 27.7 mm. This should lead to a reduction in the strength because the cooling rate when rolling is completed will be lower for a thicker plate and because the rolling reductions occur at relatively higher temperatures (the thicker slab spends the same time in the mill). The finish rolling temperature will be higher for 27.7 mm plate compared with 13.8 mm plate. The reduction in strength is predicted by the neural network, as shown in Fig. 11, although there is some uncertainty due to the large error bars for the UTS calculations. It needs to be emphasised that an initial slab thickness of 400 mm is



11 Effect of plate thickness on *a* YS and *b* UTS of niobium microalloyed steel as function of carbon concentration

simply used as an example here to test the model predictions. In actual practice, the initial slab thickness is typically in the range 225–305 mm. Alternatively, an ingot of an initial thickness of 600 mm is used.

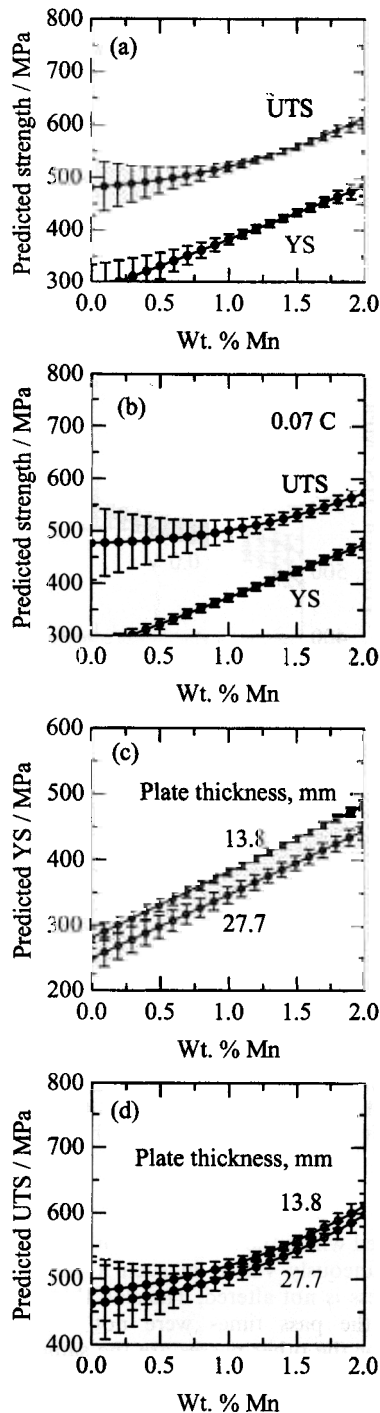
Manganese concentration

Manganese not only provides solid solution strengthening, but also has a strong effect on the stability of the austenite. It decreases the ferrite transformation temperature and therefore leads to a refinement of microstructure.¹⁷ Manganese also shifts the eutectoid point to lower carbon concentrations and thus leads to an increase in the volume fraction of pearlite.

The Pickering equations given above¹⁰ attribute a 32 and 27 MPa solid solution strengthening increment in the yield and ultimate tensile strengths, respectively, due to a 1 wt-% increase in the manganese level. The predictions in Fig. 12*a* and *b* include all the effects of manganese and hence the somewhat larger strength increment is consistent with the smaller values reported by Pickering. The results are in agreement with the work of Gladman *et al.*¹⁸ for a normalised steel.

As with carbon, an increase in the plate thickness led to a decrease in strength (Fig. 12*c* and *d*). The increase in thickness was achieved by doubling the slab thickness while keeping the same rolling schedule. The reduction in the yield strength is larger than in the UTS, presumably because the former is more sensitive to grain size (equations (7) and (8)).

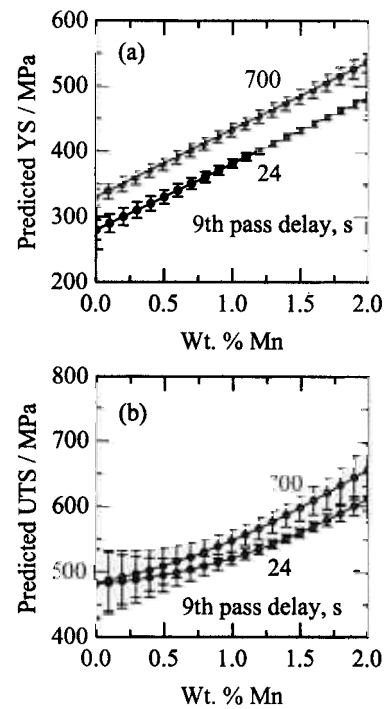
It is a common practice during thermomechanical processing to hold the slab at an intermediate stage during rolling for a certain length of time. This allows it to cool to a predetermined temperature before rolling is resumed. The temperature is then sufficiently low to prevent the austenite from recrystallising during deformation. The deformation and the increase in austenite surface area per unit volume due to its pancake shape enhances the ferrite nucleation rate, giving grain refinement and a



12 *a, b* YS and UTS as function of manganese content and *c, d* effect of manganese concentration and plate thickness on strength; thickness was increased by doubling initial slab thickness

corresponding increase in strength. This behaviour is predicted as illustrated in Fig. 13. The delay period before the 9th pass was increased from 24 to 700 s; this would have the effect of reducing both the end hold temperature and the finish rolling temperature with a consequent increase in the yield and tensile strengths (Fig. 13).

If the increase in the strength is assumed to be due to grain refinement, then, according to the Pickering regression equations (7) and (8), the increase in YS should be 1.13/0.5 times the rise in UTS. The model predictions are in excellent agreement with this. For a 1.3 wt-%Mn steel the YS increases by 52 MPa, whereas UTS increases by 23 MPa (Fig. 13). Thus, it might be argued that a delay of 700 s



13 Effect of delay period before 9th pass on strength for range of manganese concentrations

before the 9th pass is equivalent to an addition of about 0.025 wt-% of costly niobium. These factors are consistent with the mill experience though, in actual practice, it is the concentration of carbon and/or manganese which is reduced rather than that of niobium to improve the weldability and toughness. However, a hold of as large a period as 700 s has other commercial implications. It amounts to a total loss of production; in 700 s two plates can be rolled to schedules which do not involve long delay periods.

The calculations carried out for manganese were repeated for silicon in concentrations up to 1 wt-%, but it was found not to have any significant effect on the strength. Silicon raises the ferrite transformation temperature and this might compensate for its solid solution strengthening.

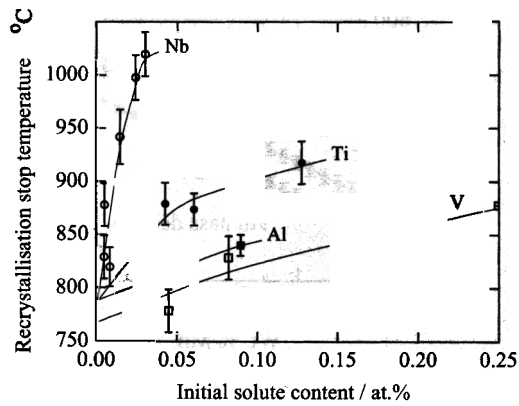
Microalloying additions

Niobium and vanadium carbonitrides prevent austenite grain coarsening during reheating.¹⁹ They also help refine the austenite grain structure during hot rolling by pinning the grain boundaries and retarding recrystallisation.¹⁹ Niobium is the most effective microalloying addition for suppressing the recrystallisation (Fig. 14).²⁰ This is also evident from the regression equation proposed by Boratto *et al.*²¹

$$T_{nr} = 887 + 464w_C + (6445w_{Nb} - 644w_{Nb}^{0.5}) + (732w_V - 230w_V^{0.5}) + 890w_{Ti} + 363w_{Al} - 357w_{Si} \quad (9)$$

where T_{nr} is the no recrystallisation temperature, i.e. the temperature below which recrystallisation is very sluggish and w represents the concentration (in weight per cent) of the element identified by the subscript.

By suppressing recrystallisation, they allow a higher fraction of the strain to be retained in austenite. This increases the ferrite nucleation rate during subsequent cooling and a finer ferrite grain size is obtained. Niobium is more effective than vanadium in refining the grains. Abe *et al.*¹⁶ and Irvine *et al.*¹⁵ have observed a finer ferrite grain size in niobium steel than in comparable vanadium steel. A larger concentration of vanadium is required to achieve the same effect as niobium.¹⁵ Interphase precipitation



14 Effects of microalloying elements on recrystallisation temperature of austenite in low carbon steel²⁰

also causes grain refinement by hindering the ferrite grain growth.²²

At the same grain size microalloyed steels have higher strength than the plain C-Mn steels,¹⁵ and this has been attributed to the presence of fine precipitates of carbides and nitrides of the microalloying elements. In this respect V is more effective than Nb particularly at higher nitrogen contents.²³

Both Nb and V also increase the hardenability and reduce the ferrite transformation temperature.^{16,22}

These characteristics are predicted using the neural network model as shown in Fig. 15. A 0.02 wt-% increase in Nb, in the region in which the error bars are small, increases the yield strength by about 40 MPa and the tensile strength by 25 MPa, whereas the same amount of V increases both the YS and the UTS by only 15 MPa. The experimental results reported in the literature more or less confirm these model predictions.^{12,15-17,24}

Figure 15 also highlights the fact that a combined addition of V and Nb enhances the strengthening effects, consistent with the experimental results reported by Irvine et al.¹⁵ They found that an addition of 0.06 wt-% V to a Nb microalloyed steel raises the yield strength by about 40 MPa and the UTS by a smaller increment of 15 MPa.

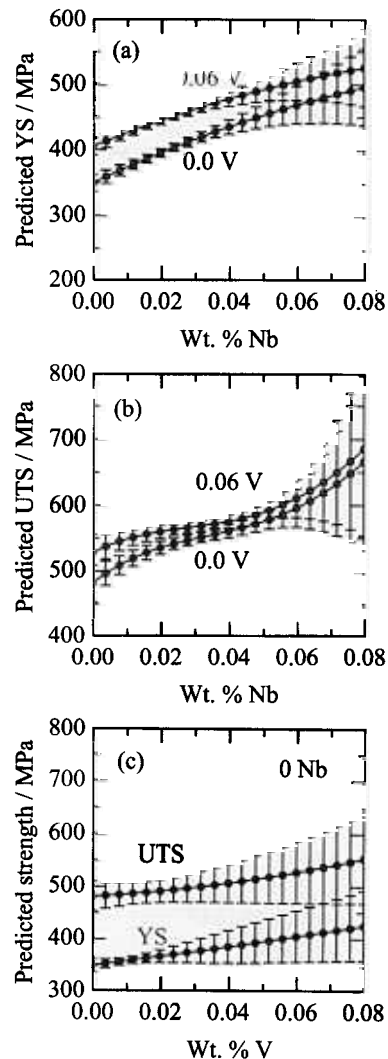
Rolling parameters

Figure 16 shows the effect of a 1st pass reduction on the yield and ultimate tensile strengths; both increase as the pass reduction is increased, with the yield strength showing a greater variation. Figure 16 is an extrapolation over the normal rolling practice. Usually the 1st pass reduction is less than 10% and in some cases it may be preceded by a few unrecorded cogging passes. It should also be noted that the effect shown in Fig. 16 is not of the pass reduction alone. Other factors need to be taken into account. The percentage reduction in all other passes were kept constant so that, for a given slab thickness, a higher 1st pass reduction meant a lower gauge at all other stages of rolling and hence a thinner final plate gauge. It follows that with increasing 1st pass reduction all other subsequent passes are executed at lower temperatures due to the thinner gauge.

The effect of increasing (i) the initial slab thickness to 400 mm and (ii) the 9th pass delay time (delay before 9th pass) to 500 s from 24 s is also included in Fig. 16. A slab thickness of 400 mm is used here as an example only.

The effect of increasing the slab thickness to 400 mm without changing the pass reductions is to decrease the strength, which is reasonable. For reasons already discussed, the introduction of the delay period of 500 s before the 9th pass increases the strength.

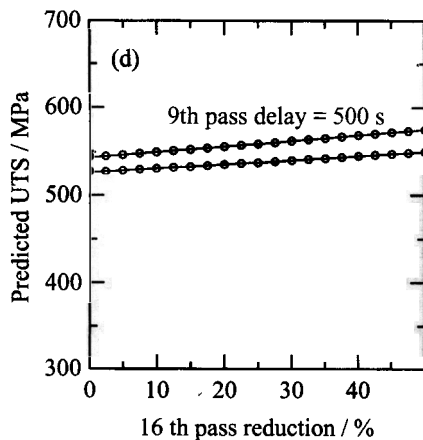
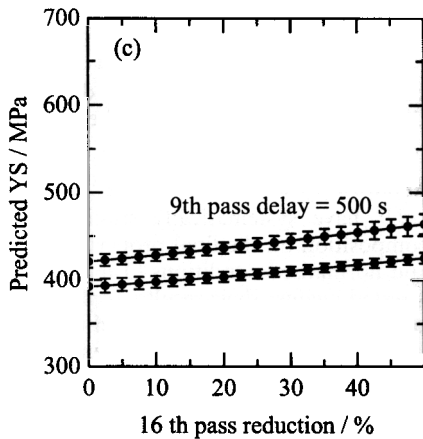
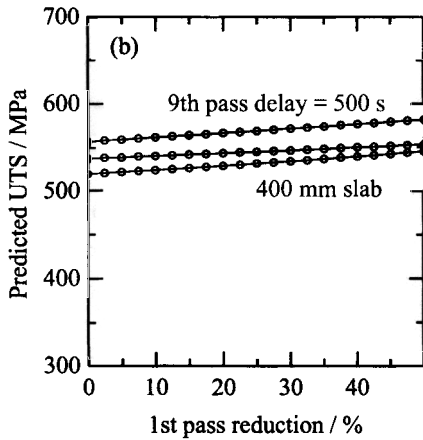
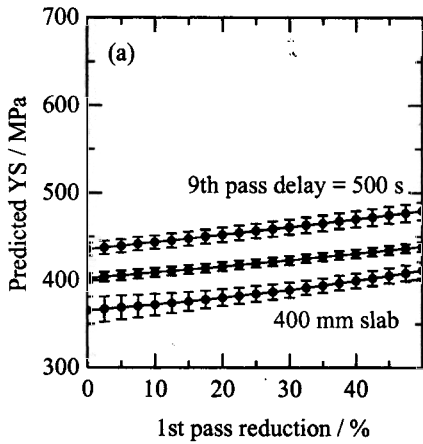
In the above discussion, the per cent reduction of only one pass was systematically varied. This has the effect of changing the final plate thickness. Some calculations are



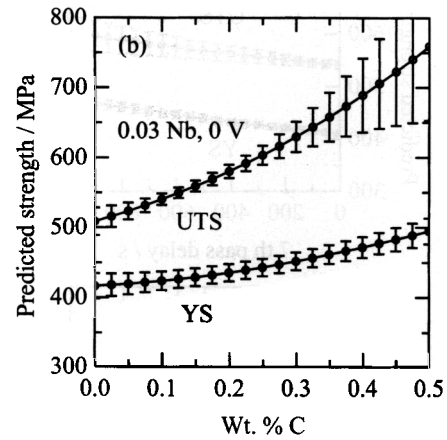
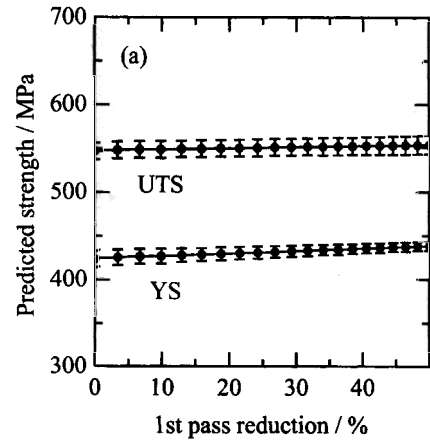
15 Effect of Nb and V on yield and tensile properties (normally V is not added alone but is combined with Nb); calculations are presented here for illustration only

now presented where the reductions for two or more passes were simultaneously varied in such a way that the final plate thickness is not altered. The slab thickness, the delay times, and the pass times were not changed and the reductions for the other passes are the same as in Table 2. Figure 17a shows the lack of variation in strength for a case where the 1st pass reduction was increased together with a corresponding decrease in the 19th (final) pass reduction which left the final plate thickness unaltered at 8.1 mm for a 200 mm starting slab. This is because a small 1st pass reduction leads to a higher temperature for all subsequent passes including the final pass with a high reduction since none of the delay times is altered, so that the strength does not increase. When the 1st pass reduction is large, the later passes occur at a lower temperature. It is suggested that the resultant of these two effects is that the strength does not vary.

Similar results were obtained when the schedule given in Table 2 was modified. The 15th and 16th pass strains were set to zero, but the 4th and 5th pass strains were increased equally so that the final plate thickness remained 13.8 mm. The effect of this change in schedule on the variation of YS and UTS with carbon is shown in Fig. 17b. A comparison with Fig. 10a makes it obvious that the change in schedule has not made much of a difference to the properties.



16 a, b Effect of 1st pass reduction on YS and UTS and c, d corresponding effects as function of 16th pass reduction



17 a Effect of simultaneous variation of first and last pass strain keeping final plate thickness constant and b effect of modification of schedule given in Table 2 such that final plate thickness was same

It has already been seen that the introduction of a delay time can have an effect on the final mechanical properties if it leads to grain refinement. Naturally, this can only be significant at the late stages of rolling and this is reflected in the results shown in Fig. 18.

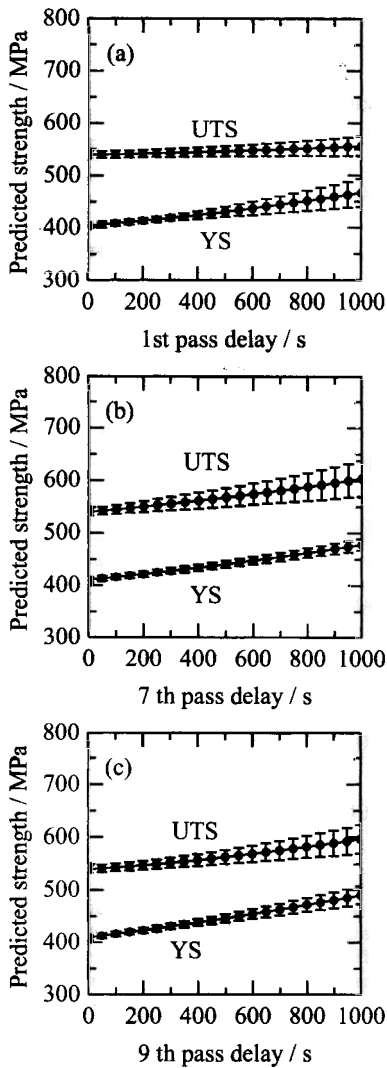
Optimisation of YS/UTS ratio

The YS/UTS ratio is an important design criterion for many failsafe applications where a low value is desired. Examples include earthquake resistant steels and cases where a good fatigue resistance is required.²⁵

The present model was used to explore the possibility of designing such a steel. The effect of variations in the carbon and manganese concentrations on the ratio are summarised in Fig. 19.

Table 3 Chemical composition, wt-%, of steels studied by Irvine et al.¹⁵

Steel	C	Mn	Si	Al	N	Nb	V
1	0.10	0.60	0.41	0.08	...
2	0.10	0.50	0.1	...	0.013	...	0.095
3	0.15	1.39	0.22	0.039	0.015
4	0.05	1.30	0.09	...	0.0072	0.037	...
5	0.044	1.42	0.24	...	0.0088	0.048	0.058
6	0.099	1.35	0.26	...	0.0076	0.044	...
7	0.104	1.43	0.27	...	0.0080	0.047	0.075
8	0.151	1.48	0.27	...	0.0080	0.047	...
9	0.149	1.49	0.32	...	0.0088	0.049	0.070
10	0.046	1.40	0.27	...	0.0138	0.037	...
11	0.040	1.31	0.26	...	0.0172	0.043	0.072
12	0.083	1.32	0.16	...	0.016	0.03	...
13	0.085	1.36	0.13	...	0.0154	0.04	0.070
14	0.148	1.43	0.23	...	0.0142	0.04	...
15	0.144	1.48	0.22	...	0.0144	0.05	0.08

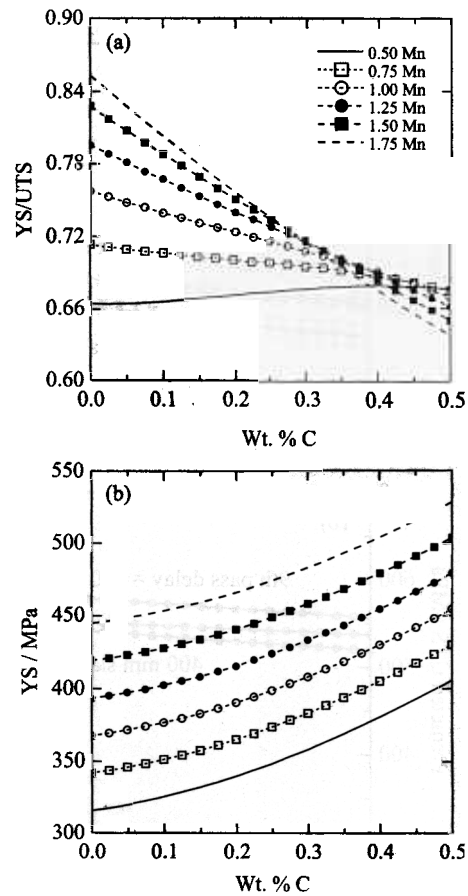


18 Effect of delay time on YS and UTS

The ratio decreased with increasing carbon concentration. As argued earlier, this is because the pearlite content increases with carbon which affects UTS more than the YS. However, a very high carbon is not acceptable because of its adverse effect on weldability and toughness. Low carbon will not give adequate strength. Manganese raises the ratio mainly due to its influence on ferrite grain size which raises the YS more than the UTS. Other factors

Table 4 Comparison of predicted yield (YS) and tensile (UTS) strengths with those reported in literature¹⁵

Steel	YS, MPa		UTS, MPa	
	Measured	Predicted	Measured	Predicted
1	469.5	419.5	568.2	
2	335.0	368.7	427.7	
3	328.9	355.4	528.0	
4	370.7	417.7	457.0	
5	457.2	497.3	568.2	
6	420.0	443.4	555.8	
7	488.0	513.6	617.6	
8	432.4	468.4	599.1	
9	488.0	522.7	660.8	
10	401.5	430.0	524.9	
11	457.1	494.4	543.5	
12	413.9	409.4	537.3	
13	457.1	498.0	574.4	
14	444.8	449.5	611.4	
15	512.8	536.1	660.8	



19 Effect of carbon and manganese on YS/UTS ratio and YS

which affect the YS/UTS ratio are the delay period and the plate thickness. These have already been discussed.

Other published data

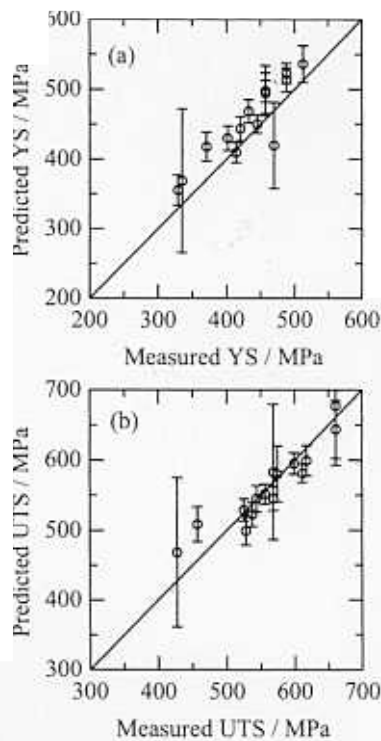
Irvine et al.¹⁵ have systematically studied the effect of chemical composition on the final properties of steel in the as rolled and normalised conditions (Table 3). The present model was tested against their results. In their experiments the samples were reheated to 1200°C and the finish rolling temperature was about 900°C. They have not reported the details of rolling schedule employed and for the present calculation it has been assumed that they are similar to the standard conditions used here. It is clear that the model predicts the data rather well (Fig. 20 and Table 4).

CONCLUSIONS

A neural network model capable of predicting the yield and tensile strengths of steel plates as a function of composition and rolling parameters has been trained and tested. The model has been shown to be consistent with established metallurgical trends and can, for example, be used to study the effect of each variable in isolation. There are interesting results on the yield strength/tensile strength ratio whose value can be altered systematically by controlling the carbon and manganese concentrations.

ACKNOWLEDGEMENTS

The authors are grateful to British Steel plc for financial support and to Dr K. Melton, Research Director, Swinden Technology Centre for permission to publish this paper. They also thank Professor A. H. Windle for the provision of laboratory facilities at the University of Cambridge, and



20 Comparison of predicted YS and UTS with experiments reported in literature¹⁵ (note that these experiments were not included in training database)

Mr J. Street for his help in setting up the database required for the analysis. One of the authors (SBS) thanks Cambridge Commonwealth Trust for a scholarship.

REFERENCES

1. T. GLADMAN: 'The physical metallurgy of microalloyed steels'; 1997, London, The Institute of Materials.
2. D. J. C. MacKAY: 'Mathematical modelling of weld phenomena 3', (ed. H. Cerjak and H. K. D. H. Bhadeshia), 359; 1997, London, The Institute of Materials.
3. D. J. C. MacKAY: *Neur. Comput.*, 1992, 4, 415.
4. D. J. C. MacKAY: *Neur. Comput.*, 1992, 4, 448.
5. D. J. C. MacKAY: *ASHRAE Trans.*, 1994, 100, (2), 1053.
6. D. J. C. MacKAY: *Network: Computat. Neur. Systems*, 1995, 6, 469-505.
7. H. K. D. H. BHADESHIA, D. J. C. MacKAY, and L.-E. SVENSSON: *Mater. Sci. Technol.*, 1995, 11, 1046.
8. R. M. NEAL: 'Bayesian learning for neural networks'; 1996, Berlin, Springer Verlag.
9. R. W. K. HONEYCOMBE and H. K. D. H. BHADESHIA: 'Steels: microstructure and properties'; 1995, London, Edward Arnold.
10. F. B. PICKERING: 'Physical metallurgy and the design of steels'; 1978, London, Allied Science Publishers.
11. P. D. HODGSON and R. K. GIBBS: *ISIJ Int.*, 1992, 32, 1329.
12. M. SHIMIZU, M. HIROMATSU, S. TAKASHIMA, H. KAJI, and M. KANO: 'HSLA steels: metallurgy and application', (ed. J. M. Gray et al.), 591; 1986, Metals Park, OH, ASM.
13. W. C. LESLIE: 'The physical metallurgy of steels'; 1981, New York, McGraw-Hill Book Co.
14. W. B. MORRISON: *Trans. ASM*, 1966, 59, 824.
15. K. J. IRVINE, F. B. PICKERING, and T. GLADMAN: *J. Iron Steel Inst.*, 1967, 210, 161.
16. T. ABE, K. TSUKADA, and I. KOZASU: 'HSLA steels: metallurgy and application', (ed. J. M. Gray et al.), 103; 1986, Metals Park, OH, ASM.
17. M. COHEN and S. S. HANSEN: 'HSLA steels: metallurgy and application', (ed. J. M. Gray et al.), 61; 1986, Metals Park, OH, ASM.
18. T. GLADMAN, D. DULIEU, and I. D. McIVOR: 'Microalloying 75', (ed. M. Korchynsky), 25-32; 1977, New York, Union Carbide Corp.
19. R. K. AMIN and F. B. PICKERING: 'Thermomechanical processing of microalloyed austenite', (ed. A. J. DeArdo et al.), 1; 1981, Warrendale, PA, TMS-AIME.
20. L. J. CUDDY: 'Thermomechanical processing of microalloyed austenite', (ed. A. J. DeArdo et al.), 129; 1981, Warrendale, PA, TMS-AIME.
21. F. BORATTO, R. BARBOSA, S. YUE, and J. J. JONAS: 'Physical metallurgy of thermomechanical processing of steel and other metals (Thermec-88)', (ed. I. Tamura), 383; 1988, Tokyo, ISIJ.
22. R. K. AMIN and F. B. PICKERING: 'Thermomechanical processing of microalloyed austenite', (ed. A. J. DeArdo et al.), 377; 1981, Warrendale, PA, TMS-AIME.
23. K. J. IRVINE, and F. B. PICKERING: *J. Iron Steel Inst.*, 1963, 201, 944.
24. J. LESSELLS: 'HSLA steels: metallurgy and application', (ed. J. M. Gray et al.), 613; 1986, Metals Park, OH, ASM.
25. H. K. D. H. BHADESHIA: 'Bainite in steels'; 1992, London, The Institute of Materials.